

Observations of Liquid Water in Orographic Clouds over Elk Mountain

MARCIA K. POLITOVICH AND GABOR VALI

Department of Atmospheric Science, University of Wyoming, Laramie 82071

(Manuscript received 20 April 1982, in final form 13 December 1982)

ABSTRACT

The relatively simple orographic clouds forming in winter over Elk Mountain, Wyoming, provided useful opportunities for field studies of cloud formation and of ice crystal development. In this paper, the observations of cloud droplet populations, spanning a range of five consecutive years, are summarized.

Data are presented which describe the climatology of the cloud droplet spectra. Selected cases are described in detail to illuminate the processes at work and to allow comparisons with theoretical predictions.

Droplet concentrations are mostly around 300 cm^{-3} in accordance with the weak updrafts of the clouds and with the mid-continental, unpolluted cloud condensation nucleus concentrations prevailing in the region. In general, the data are in agreement with one-dimensional microphysical model calculations.

1. Introduction

For a little more than a decade we have been collecting measurements in the wintertime cap clouds which form over Elk Mountain, Wyoming. The relatively simple airflow structure of these clouds, their temporal stability and accessibility for both surface and airborne observations make these clouds attractive for studies of certain fundamental cloud microphysical processes. The origin of ice in these clouds has been given the greatest emphasis in our studies. Results related to that question are given in other papers (e.g., Saunders, 1978; Cooper and Vali, 1981). In this paper, we present the general characteristics of the liquid cloud.

The description to be presented here is intended to document the liquid cloud characteristics and their ranges of variation, to examine the factors responsible for the observed properties of the clouds, and to view the processes in the light of general theories of cloud formation.

Other studies of orographic clouds and storms, including those of the San Juan Mountains of Colorado, have been conducted by the Universities of Wyoming (Cooper and Marwitz, 1980) and Washington (Hobbs and Atkinson, 1976). The main difference between those studies and the present one is that the clouds studied over Elk Mountain constitute a more narrowly-defined and more extensive set. No important contradictions emerge between ours and the other studies of orographic clouds.

2. Site and instruments

Elk Mountain is an isolated peak at the north end of the Medicine Bow Range in southeastern Wyo-

ming. It rises from the Saratoga Valley to the west, at ~ 2.2 km, to a height of 3.38 km (all heights are MSL except when AGL is specified). The meteorological Observatory is at 3.29 km and is located in a depression between the main summit to the east and a slight ridge to the west (3.35 km). The Observatory is equipped for measuring and recording temperature, humidity, and wind velocity (both at the Observatory and the ridge to the west), as well as water droplet and ice particle spectra and the liquid water content.

For studies of the cloud and its environment, the University of Wyoming Queen Air research aircraft (N10UW) was used. This aircraft was equipped for measurements of state parameters and for *in situ* measurements of cloud particle number concentrations, sizes, shapes and phase.

Of specific interest in this paper are the instruments used for cloud particle and liquid water content measurements (see Table 1).

The instrument in longest continuous use at the observatory is the impactor slide sampler or "cloud gun" (CG) which is fashioned after the device designed by Squires and Gillespie (1952). A small CO_2 -powered gun shoots a soot-coated glass or plastic slide past an aperture where it is exposed to the airstream (at the Observatory a vacuum pump is used to draw air past the aperture at about 33 m s^{-1}). Each droplet impacting onto the soot-coated surface leaves a permanent crater-like impression the diameter of which is related to the impact speed and droplet size. The impressions are photographed and their size distribution is used along with the airspeed and exposure time to calculate the droplet size spectrum, relying on empirical calibrations of crater size to droplet size ratios.

TABLE 1. Instrument parameters.

Parameter measured	Instrument type	Manufacturer	Range (μm)	Resolution (μm)	Sample volume (cm^3)	Sampling time
Cloud droplets	Impaction and replication	University of Wyoming	≥ 4 diameter	0.5–2	10 (EMO) 30 (N10UW)	5 ms
	Optical scattering	Axially Scattering Spectrometer Probe (ASSP) Particle Measuring Systems, Inc. (PMS) Boulder, CO	$\left\{ \begin{array}{l} 0.5\text{--}7.5 \\ 1\text{--}15 \\ 2\text{--}30 \\ 3\text{--}45 \end{array} \right.$	$\left\{ \begin{array}{l} 0.5 \\ 1 \\ 2 \\ 3 \end{array} \right.$	10 (EMO)	1 s (EMO)
					30 (N10UW)	0.1 s (N10UW)
	Optical scattering	PMS Forward Scattering Spectrometer Probe (FSSP)	—same as for ASSP—		5	15 s
Liquid water	Mass rime rate	Metronics Assoc. Inc., Roto-rod		$\sim 0.01 \text{ g m}^{-3}$	0.5–3 m^3	2–15 min
Ice crystals	Shadow imaging	PMS 2D-C probe	25–800 diameter	25	$\sim 0.75 \text{ l s}^{-1}$ (EMO) $\sim 4 \text{ l s}^{-1}$ (N10UW)	
	Direct sampling by collection microscope examination	University of Wyoming	≥ 10 diameter	—	$\sim 5 \text{ l s}^{-1}$ (EMO) $\sim 9 \text{ l s}^{-1}$ (N10UW)	2–10 s 1–30 s
Aitken particles	Expansion chamber	Environment One, Inc. Model Rich 100	$> 50 \text{ \AA}$	NA	50	1 s

The Axially Scattering Spectrometer Probe (ASSP) and Forward Scattering Spectrometer Probe (FSSP) count and size droplets by means of light scattering. Complete descriptions of these instruments are given by Knollenberg (1981). At the Observatory these instruments are mounted in a wind tunnel that rests diagonally along the stairway to an observation platform that is 5 m AGL. Air is drawn through the tunnel at $22 \pm 4 \text{ m s}^{-1}$. Cloud gun samples at the observatory were taken from the observation platform near the entrance to the wind tunnel. The CG aboard N10UW was extended ~ 1 m from a window near the middle of the fuselage.

The rime rod is a device used for measuring liquid water content in a supercooled cloud (Rogers *et al.*, 1983). Briefly, it consists of an H-shaped wire which is rotated rapidly about a central vertical axis. The liquid water content of the cloud, integrated over a typical sample period of 2–15 min, is calculated from the mass of accumulated rime. The rime rod is mounted on a pole which extends 2 m above the roof of the Observatory (7 m AGL).

All of these instruments have been extensively calibrated and cross-compared (cf., Baumgardner and Vali, 1981). Nonetheless, accuracies of the measurements are somewhat limited. For example, Fig. 1 shows a comparison of droplet concentrations derived from cloud gun data with those from the optical scattering probes. It is evident that differences of a

factor of 2 or greater are not uncommon, but a substantial (though unknown) fraction of this variability is a result of differences in sampling locations, and in sample volumes. Absolute accuracies of the measurements cannot be clearly established. From the studies referred to earlier, it was found that droplet concentrations are accurate to approximately $\pm 30 \text{ cm}^{-3}$, droplet diameters to $\pm 2 \mu\text{m}$, and liquid water contents to \pm a factor of 2. We have found that liquid water contents measured by the rime rod method agree very well with theoretical calculations as well as with values derived from the CG and ASSP.

3. The cap cloud and its environment

a. Synoptic and local influences

Between November and April, Elk Mountain is covered by clouds about one of every three days. The formation of these orographic clouds requires certain combinations of stability, wind speed and moisture.

The most common synoptic feature present when orographic clouds form over Elk Mountain is passage of an upper level disturbance, or short wave, seen at the 500 mb level. These short waves are usually distinguished by falling barometric pressure, cold air advection and advection of moisture into the area. A surface front often accompanies the short wave. Less frequently, cloud formation is associated with shallow surface cold fronts with no associated upper

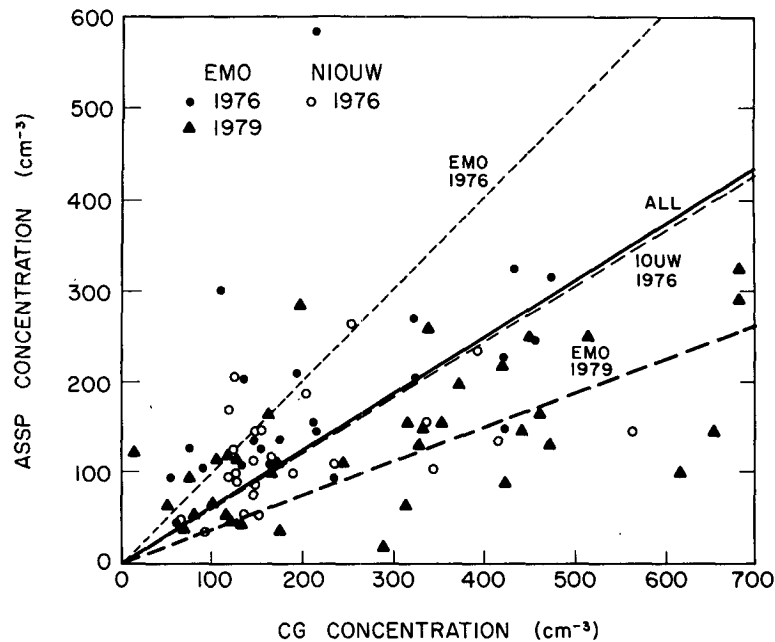


FIG. 1. ASSP or FSSP-measured droplet concentrations plotted against simultaneous CG measurements. The optical probe data are 1 s values, CG data are typically 5–10 ms. Lines are best fit to the data, forced through the origin.

level disturbance, or with surface upslope winds (NE through SE).

Elk Mountain is on the southern end of the so-called “wind corridor” of Wyoming, where winter winds are strong and persistent. During cap cloud occurrences, surface winds near Elk Mountain are typically southwesterly at $10\text{--}20\text{ m s}^{-1}$. Winds of at least 10 m s^{-1} appear to be necessary for vertical motion sufficient for cap cloud formation to develop in addition to the horizontal divergence around the isolated peak.

Some moisture in the boundary layer is usually advected with the airmass, and is significantly augmented by snow cover on the upwind prairies. Aircraft soundings taken above the valley usually reveal a well-mixed boundary layer, topped by an inversion or stable layer near the altitude of the mountain peaks.

b. General nature of the cap clouds

We have separated the orographically-induced cloud types observed at Elk Mountain into two basic categories, cap clouds and larger orographic clouds.

Cap clouds are defined as isolated clouds which are confined to a single peak or ridge, such as the summit of Elk Mountain. Larger orographic clouds cover a greater horizontal extent; at times they may cover the entire Medicine Bow Range. We have also observed deep cloud systems which are not orographically induced, although they may contain regions altered by the mountain’s influence. These deep systems are syn-

optic in scale and are most often associated with frontal passages. They will not be addressed in this paper.

The cap and orographic clouds are typically ~ 1 km thick, ranging from several hundred meters to nearly 2 km. Cloud base heights range from 2.6 to 3.4 km and tops from 3.3 to >6 km. The upwind (usually west) edge of the cap cloud is commonly less than 2 km from the summit but may extend to ~ 7 km. Residence times of air parcels within these clouds can range from 500 to 1500 s depending on cloud extent and wind speed.

4. Climatology of clouds at the Observatory

The set of CG samples taken at the Elk Mountain Observatory constitute a fairly large, and consistent data set which can be used to examine the average properties and variabilities of cloud droplet populations. These samples were taken selectively, when the observers judged the clouds enveloping the Observatory to be homogeneous and steady. The set, useful for establishing climatological values, consists of 89 samples taken on 18 days, spread over four years.

Table 2 lists the major characteristics derived from the cloud gun samples. Average values and standard deviations from the sample sets are listed.

The droplet concentrations are given per cm^3 of air at the 680 mb altitude of the Observatory. Average droplet concentrations range from 250 to 350 cm^{-3} , and there is relatively little difference between cloud types. Essentially all samples had concentrations $<500\text{ cm}^{-3}$. The mean diameters of the spectra are

TABLE 2. Summary of cloud droplet characteristics at the Observatory.

	Cap clouds	Larger orographic clouds	Combined
Concentration N (cm^{-3})	$295 \pm 180^*$	241 ± 159	275 ± 175
Mean diameter \bar{d} (μm)	8.9 ± 2.3	11.3 ± 4.0	9.8 ± 3.2
Dispersion	0.16 ± 0.05	0.17 ± 0.04	0.16 ± 0.05
Liquid water content (g m^{-3})	0.15 ± 0.18	0.29 ± 0.38	0.20 ± 0.28
Average temperature of observations ($^{\circ}\text{C}$)	-12.2 ± 3.1	-10.8 ± 2.5	-11.7 ± 3.0
Number of samples (days)			
January	34 (4)	28 (4)	62 (8)
February	14 (6)	5 (1)	19 (7)
April	8 (3)	—	8 (3)
Total	56 (13)	33 (5)	89 (18)

* The standard deviation of the sample set is given for each parameter.

close to $10 \mu\text{m}$; this small size reflects the small amount of lifting from the upwind cloud edge to the Observatory.

An important characteristic of the droplet spectra is their narrowness. Dispersions (standard deviation of the spectrum divided by mean diameter) range between 0.1 and 0.3, the group averages for cap and orographic clouds being 0.16. Such narrow droplet

spectra are expected to result from condensation without the broadening effects of coalescence or by mixing of different air parcels. A few examples of droplet spectra are given in Fig. 2.

The liquid water contents (LWC) of the clouds at the Observatory vary quite widely because of variations in cloud base altitude and inhomogeneities in the cloud. Here LWC up to 1 g m^{-3} were occasionally observed, but, as Table 2 shows, the mean values are considerably lower, 0.15 g m^{-3} for the isolated cap clouds and 0.29 g m^{-3} for the larger orographic clouds. The complete set of LWC data from the cloud gun samples is shown in Fig. 3 plotted against temperature. For reference, the adiabatic LWC corresponding to different assumed cloud thicknesses below the observatory are also shown. While the rough agreement between the higher measured values and the adiabatic values is perhaps meaningful, these data do not permit conclusions to be drawn concerning the degree of mixing in the cloud, mainly due to a lack of cloud base information corresponding to each of the LWC measurements. Fig. 3 also shows LWC data from the rime-rod samples. Because of relatively long sampling times, the maximum values are lower than for instantaneous cloud gun samples. A combination of all rime-rod samples from cap and orographic clouds yields the frequency distribution shown in Fig. 4. As this figure represents a large total sampling period, it can be useful for describing the LWC values which contribute to the rime accumulation, and hence the water storage, on trees and other objects at the mountain surface. To demonstrate the

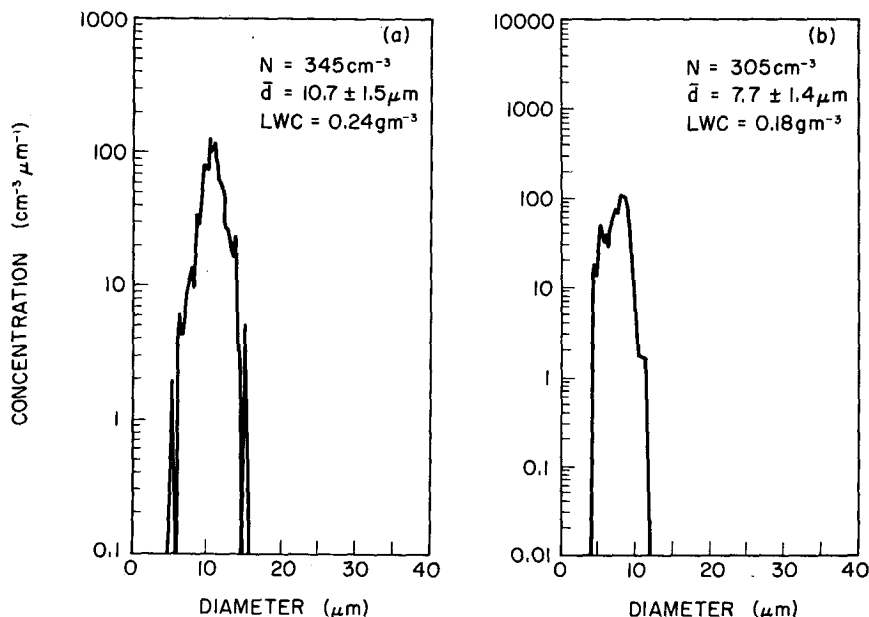


FIG. 2. Typical droplet spectra measured from the Elk Mountain Observatory for different cloud types: (a) cap cloud, (b) larger orographic cloud. Data are from CG samples.

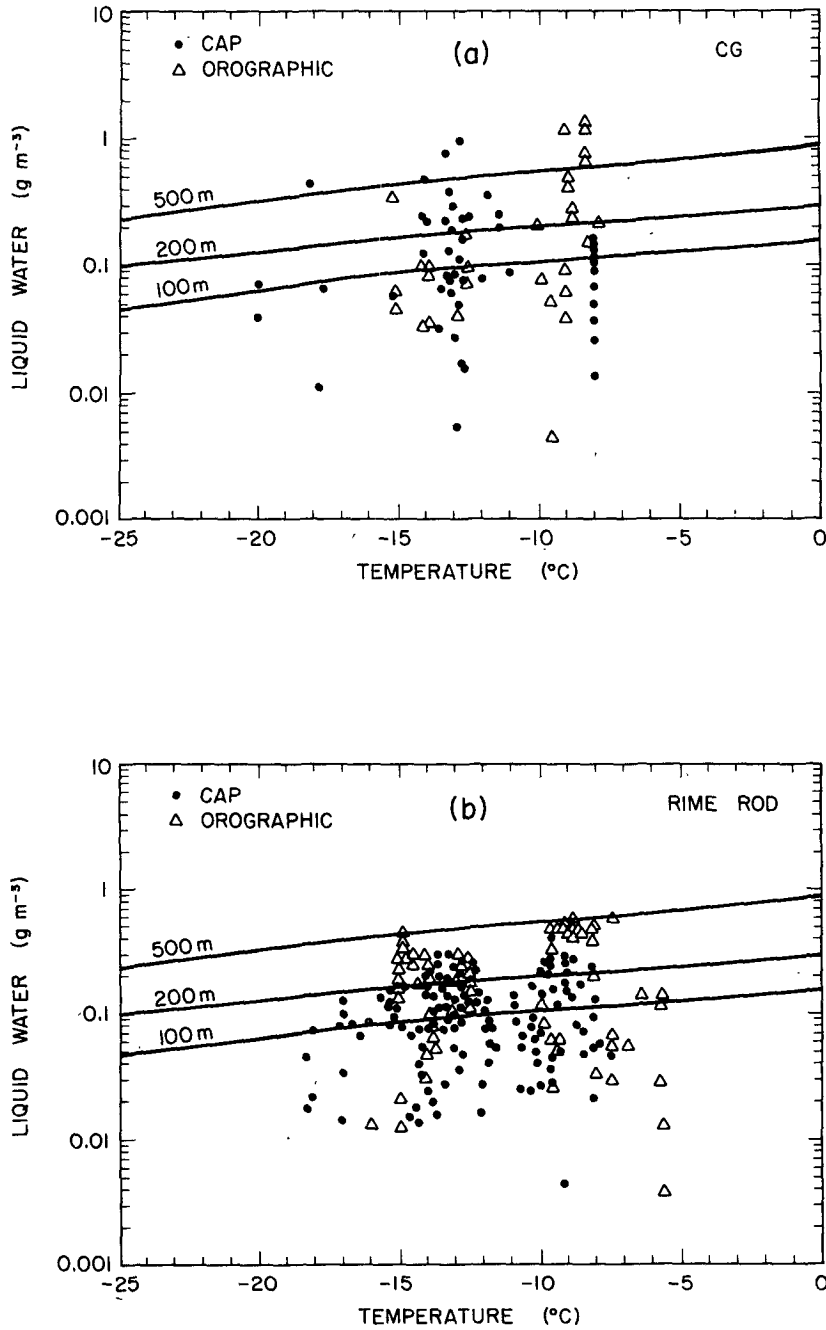


FIG. 3. Liquid water content measured from the Observatory plotted against temperature during sampling. (a) CG, (b) rime rod.

importance of rime buildup, Fig. 5 shows two examples of such rime deposits on trees near the mountain top and on the aircraft.

The preceding data referred to the characteristics of the liquid water cloud at the mountain top. These data may be influenced to some extent by the rapid rise of air along the mountain surface and possibly by removal of cloud droplets due to riming onto trees,

etc. Indications of possible biases were examined in comparisons of Observatory and aircraft data. Near-simultaneous observations of droplet spectra were made on eight days involving different combinations of instruments. These data exhibited considerable variability; *e.g.*, within a factor of two for droplet concentrations (see Fig. 6). These differences, however, are approximately of the same magnitude as

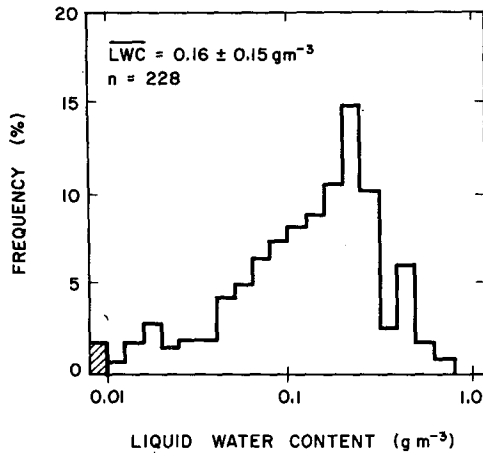


FIG. 4. Frequency histogram (plotted in logarithmic intervals) of liquid water contents at the Observatory measured with the rime-rod in cap and orographic clouds. The shaded area represents measurements $< 0.01 \text{ g m}^{-3}$.

those we found by comparing different instruments side by side (e.g., Fig. 1). Thus, no systematic influence of the mountain surface on the droplet spectra at the observatory can be discerned.

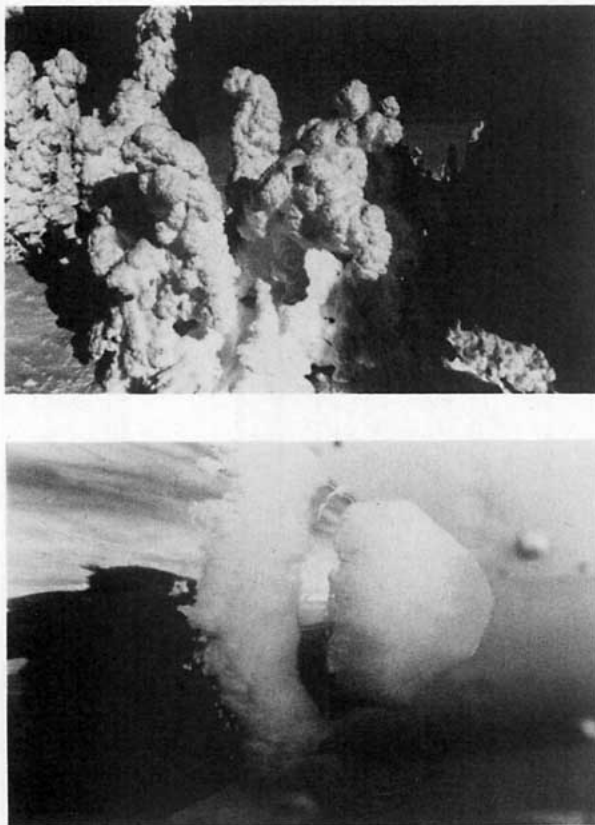


FIG. 5. Examples of rime formations frequently observed as a result of clouds over Elk Mountain. (Top) trees near summit. (Bottom) aircraft riming.

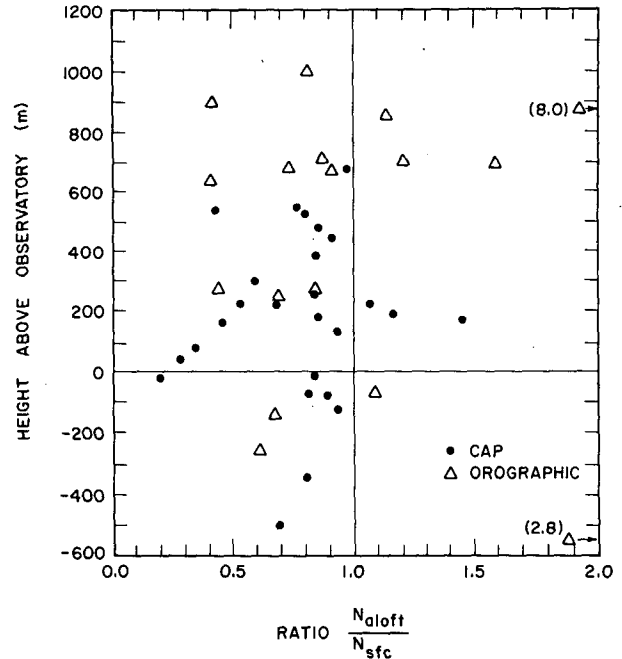


FIG. 6. Ratios of measurements from N10UW to those measured simultaneously at the Observatory. Queen Air N10UW data represent "plateau" values well into the cloud; Observatory data are ASSP values averaged over the duration of the aircraft cloud pass. Data represent our best estimates of droplet concentrations and are from CG and ASSP measurements.

5. Cloud structure

The characteristics of orographically-induced clouds observed at Elk Mountain can best be illustrated by a specific example. Our observations included a large enough number of cases to allow relatively clear, however subjective, selection of what can be viewed as "typical." Differences from this "showcase" example occur mainly in the appearance of very weak convection in some cases.

Convective bubbles or cells observed in cap and orographic clouds over Elk Mountain are small and short-lived, and their influence on the microphysical properties of the cloud is minimal. The updraft speeds are not high or persistent enough to greatly broaden the droplet spectra, but the bubbles do produce an opportunity for mixing of air parcels which results in occasionally-observed bimodal size spectra. These are most often seen near the tops of these convective bubbles and rarely at the Observatory. We have also found, as shown in Table 2, that isolated cap clouds and larger orographic clouds do not appreciably differ in their liquid water structure so that the example to be presented has quite general validity.

The cap and orographic clouds which form over Elk Mountain usually contain ice crystals. However, the ice phase generally represents a small perturbation on the properties of the liquid cloud, especially for

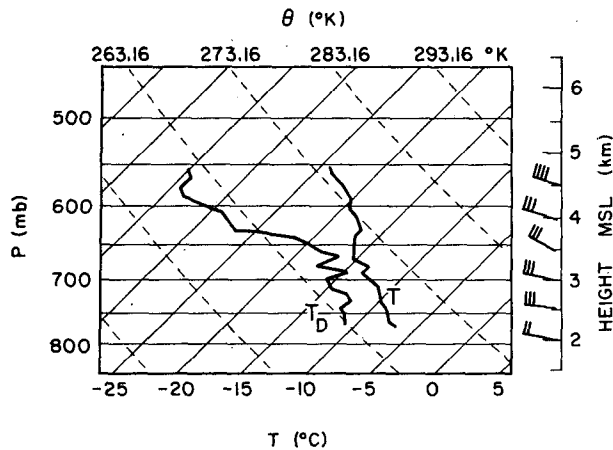


FIG. 7. Atmospheric sounding taken upwind of Elk Mountain from N10UW on 1 February 1978.

portions of the cloud where air parcels undergo ascending motions—attention will be focused on these portions in this discussion.

The case to be discussed is that of 1 February 1978. As is frequently the case for cap-cloud situations, a weak stationary front, oriented southwest–northeast, was located north of Elk Mountain that morning. The upper level flow was nearly zonal across the western United States throughout the day. A small amplitude thermal trough at 500 mb was centered over Montana and Wyoming. Winds near the surface were from the west at $\sim 15 \text{ m s}^{-1}$.

A sounding taken by N10UW at 1007–1023 MST, 25 km upwind of Elk Mountain, showed absolute stability to 4.1 km (see Fig. 7). A layer of higher relative humidities was evident between 650 and 700 mb. This is the layer in which clouds formed over the mountains.

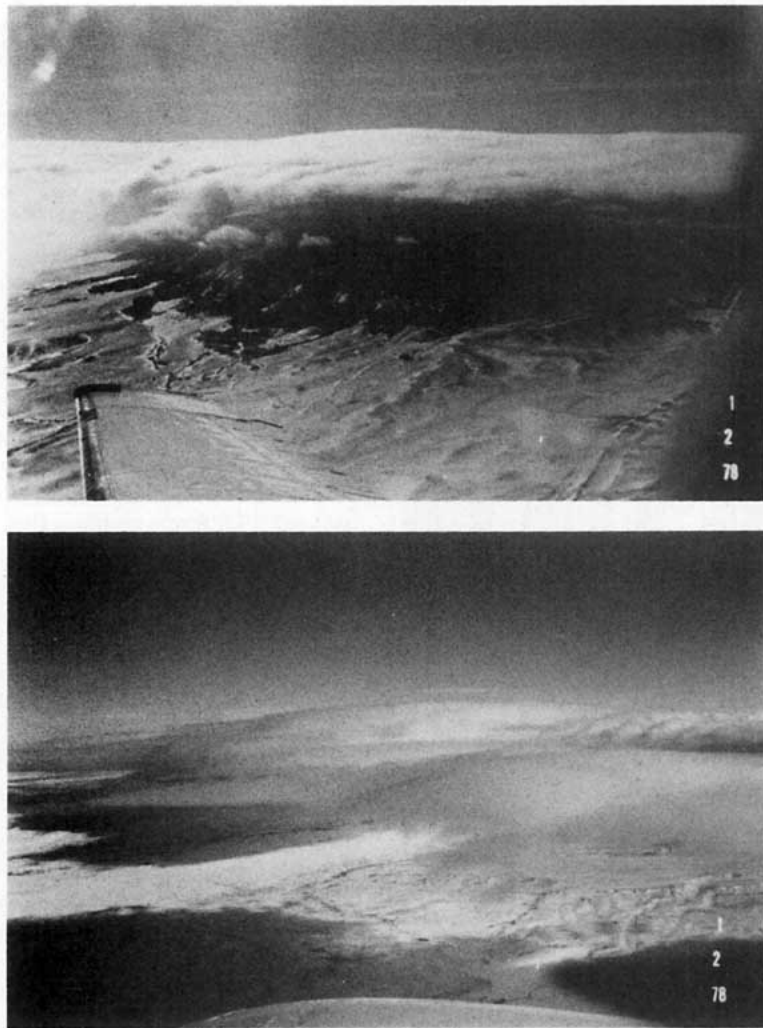


FIG. 8. Photographs taken from N10UW of the cap cloud over Elk Mountain on 1 February 1978. (Top) 1012 MST, view toward NNE. (Bottom) 1055 MST, view toward ENE.

TABLE 3. Information on N10UW cloud passes for 1 February 1978.

Pass	Time (MST)	Altitude (km)	T ($\pm \sim 1^\circ\text{C}$)	Remarks
A	1042-1046	3.5-4.0	-19	NE-SW over peak
B	1135-1138	3.5-3.9	-18	Downwind-upwind over peak
C	1202-1205	3.5-3.8	-17	Downwind-upwind over peak

Relatively shallow clouds formed over all of the Medicine Bow Range and also over the Sierra Madre Range upwind of it. Cloud bases were slightly below the altitudes of the peaks. Over Elk Mountain the cloud was somewhat thicker (~ 1 km) than elsewhere and had its leading edge ~ 8 km upwind of the mountain peak. The smooth, laminar appearance of the cloud evidenced no embedded convection. Beyond the peak, the cloud tended to break up into cellular form and evaporated within ~ 2 km in the downflow air. Figs. 8a and b show the visual appearance of the cloud. Essentially no changes in cloud features were noted over the nearly 2 h period of observations from the aircraft (roughly 1000-1200 MST), and, for several hours prior to that, conditions were observed to change little at the observatory.

Aircraft penetrations of various patterns were made to explore the cloud. For the present purposes, the most revealing penetrations are those which attempted to follow parcel trajectories through the cloud. These were made in the direction against the wind, from east to west, by entering the cloud just east of the peak near cloud-top altitude and descending so as to exit through the leading edge of the cloud. Table 3 summarizes the major aspects of three of these cloud passes. An example of the data record from such a penetration is shown in Fig. 9, with time reversed so that the positive direction of the abscissa corresponds to air parcel movement from west to east. The essential features of these data are the rapid rise and leveling-off of droplet concentrations, (at ~ 180 cm^{-3} in this case), the gradual increase in mean droplet diameter from 4 to 10 μm and the corresponding gradual increase in liquid water content. These observations are consistent with the notion that peak supersaturation is reached within a parcel shortly after the onset of condensation, and subsequently the parcel rises in a continuous fashion without substantial mixing.

The characteristics presented above can be modeled in a relatively straightforward manner. Therefore, we compared the observations with model results. However, because of a lack of detailed vertical velocity and cloud condensation nucleus (CCN) measurements the comparisons only demonstrate plausibility and do not constitute proof. The model used

was developed by Young (1974) and later revised by Kelly (1978).

Average horizontal wind speeds measured during the three cloud passes listed in Table 3 ranged from 9-17 m s^{-1} . Using an average slope value of 0.095 for the 13 km stretch upwind of Elk Mountain to the summit, resultant vertical velocities based on this geometry are 0.86-1.6 m s^{-1} . However, the effects of diffluence around the mountain, particularly with a capping inversion or stable layer act to decrease this

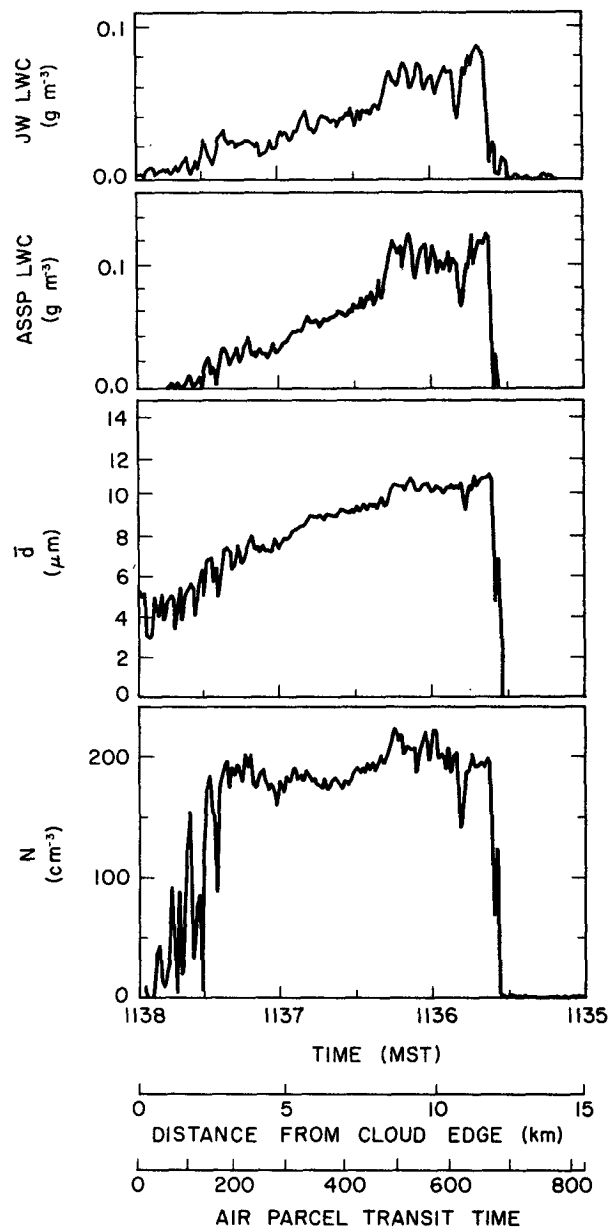


FIG. 9. Analog trace of several parameters measured from N10UW during pass "B" through the Elk Mountain cap cloud of 1 February 1978. Time (s) and distance scales (km) from cloud leading edge (based on a mean horizontal wind of 18.5 m s^{-1}) are included.

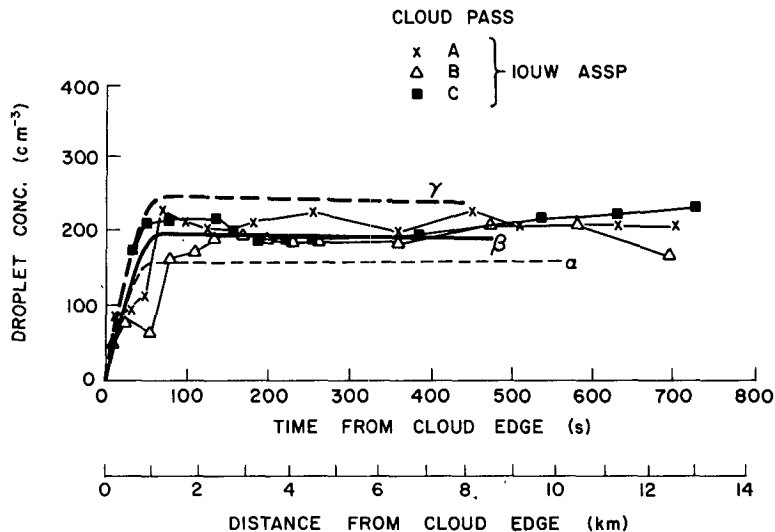


FIG. 10. Droplet concentration plotted against air parcel time and distance from the upwind cloud edge on 1 February 1978. Data are 5 s averages of ASSP measurements from N10UW. Cloud pass information is contained in Table 3. The symbols α , β and γ represent results from cloud model simulations for updraft speeds of 25, 50 and 100 cm s^{-1} .

calculated updraft. Therefore, a range of updraft values were used for model calculations which should cover those on the real cloud.

The modeled droplet concentrations as a function of time (plotted in Fig. 10) resemble the measurements from three cloud penetrations quite well. An updraft speed of 50 cm s^{-1} produced the best agreement with the data. The close agreement between the shapes of the curves suggests that the aircraft was reasonably successful in tracing air parcel trajectories.

Calculated mean droplet diameters were not in as good agreement with the data as were concentrations (see Fig. 11). The shapes of the droplet growth curves compared well with model results, but the actual mean diameters were 1–2 μm less. This is within the error of the measurements. The growth rates appeared to be approximately the same in all passes.

Total water content was derived by adding the ASSP-measured liquid water content to that calculated from 2D-C data using Davis and Auer's (1974)

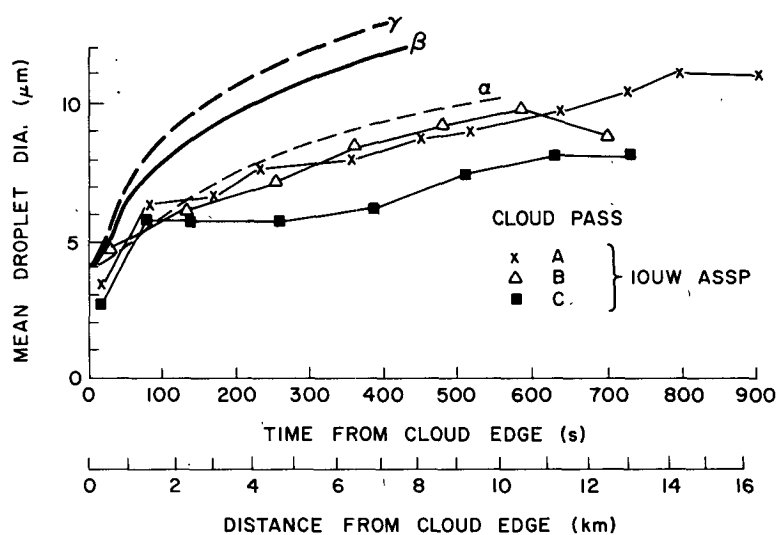


FIG. 11. Mean droplet diameter plotted against air parcel time and distance from the upwind cloud edge on 1 February 1978. Data are described in caption for Fig. 10.

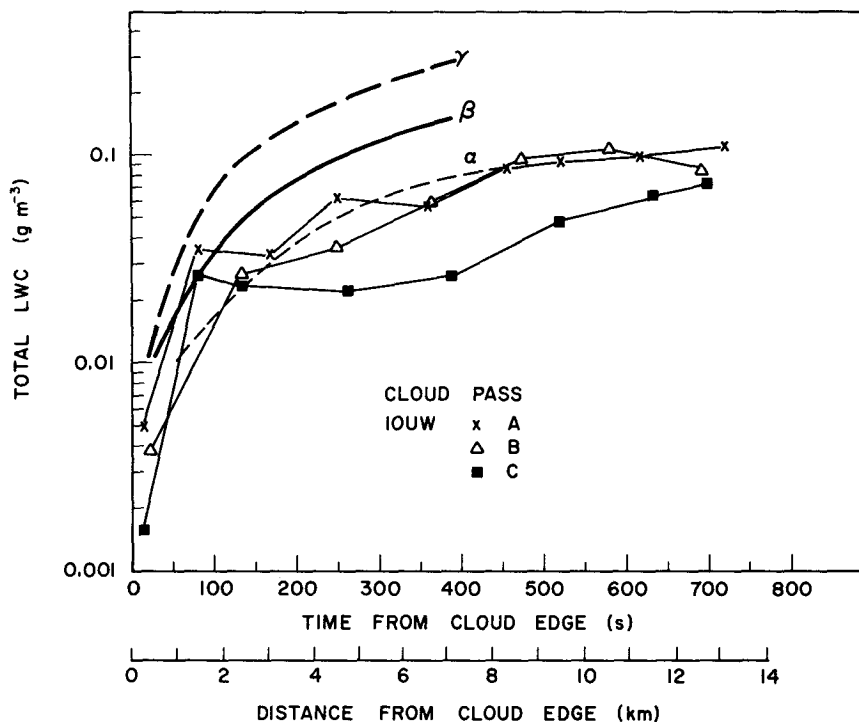


FIG. 12. Liquid water content plotted against air parcel time and distance from the upwind cloud edge on 1 February 1978. Data are described in caption for Fig. 10.

crystal diameter-to-mass relations. Ice mass concentrations were typically $<0.1 \text{ g m}^{-3}$ but occasionally attained values as high as 0.8 g m^{-3} . Total water contents are plotted against time from the upwind edge of the cloud in Fig. 12, along with predicted adiabatic values.

The liquid water contents for the three passes are somewhat below adiabatic for an updraft of 50 cm s^{-1} . Even so, with the errors involved in liquid water calculations, the uncertainties in determining the level at which the air parcel entered the cloud, and the small magnitude of the differences involved ($\leq 0.5 \text{ g m}^{-3}$), total measured liquid water contents well into the cloud aloft can probably be considered nearly adiabatic. No clear case can be made for observed water contents to be significantly below adiabatic values.

A vertical profile of the water cloud over Elk Mountain on 1 February was constructed based on a composite of aircraft (5 upwind/downwind and 4 crosswind passes) and Observatory data. Figs. 13a and b illustrate several of the main features. (The flight track from pass B is superimposed.) Droplet concentrations along an air parcel trajectory increase to reach steady levels some 1–2 km from the upwind cloud edge. The highest liquid water contents are found near the middle of the cloud, slightly upwind of the summit.

6. Cloud condensation nuclei

It is of interest to compare the cloud droplet data reported in Section 4 with cloud condensation nuclei (CCN) spectra. Measurements of CCN were made in the surface boundary layer upwind of Elk Mountain at times when clouds formed over the mountain. Because the air is usually well mixed on such occasions between the surface and the inversion which defines the cloud top, surface measurements can be taken as representative of air in which the clouds formed. The sampling sites were chosen to be well away from possible local sources of CCN.

The CCN measurements were made with a static thermal-gradient diffusion chamber equipped with photographic recording (Rogers and Politovich, 1982).

The data of interest here, extracted from a larger body of data discussed by Black (1979), are summarized in Fig. 14 in the form originated by Brahm (1974), and in Table 4. Comparison with the data of Section 4 shows that the cloud droplet and CCN data sets are compatible, if updrafts are taken to be in the range of 0.5 to 2 m s^{-1} . These values are reasonable since, for example, a 10 m s^{-1} horizontal wind would have a 0.9 m s^{-1} vertical component, when forced upward according to the average slope of the mountain.

The average values of C and k (the intercept and

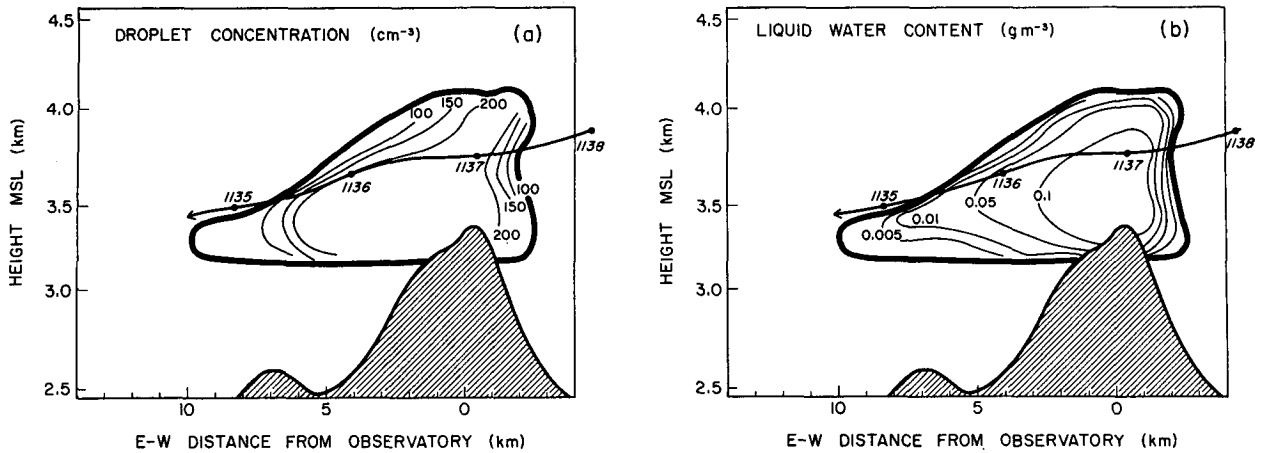


FIG. 13. Vertical structure of the cloud sampled on 1 February 1971. (a) Droplet concentration; (b) liquid water content. Flight track for pass B is also shown. Figures are based on CG and ASSP measurements from the Observatory and N10UW.

slope of the power-law equation fitted to the CCN spectra of concentration versus supersaturation described by Twomey, 1959) for the Elk Mountain data are $C = 335 \pm 116 \text{ cm}^{-3}$, and $k = 0.57 \pm 0.33$. Auer (1968) reported an average C -value of 371 cm^{-3} for winter measurements in Yellowstone National Park (~500 km NW of Elk Mountain). These wintertime data are in interesting contrast with summertime values observed in the region: $C = 900 \text{ cm}^{-3}$ and $k = 0.59$ (Rogers and Vali, 1978). The fact that the ground is snow covered in winter and that there are

no major anthropogenic sources in the region are the probable reasons for the low C -values in the winter.

7. Time variations in CCN and droplet concentrations: A case study

On 16 January 1979, an orographic cloud formed over Elk Mountain which remained there throughout the day. Droplet measurements were taken at the Observatory and surface CCN measurements were obtained from a mobile unit upwind of Elk Mountain

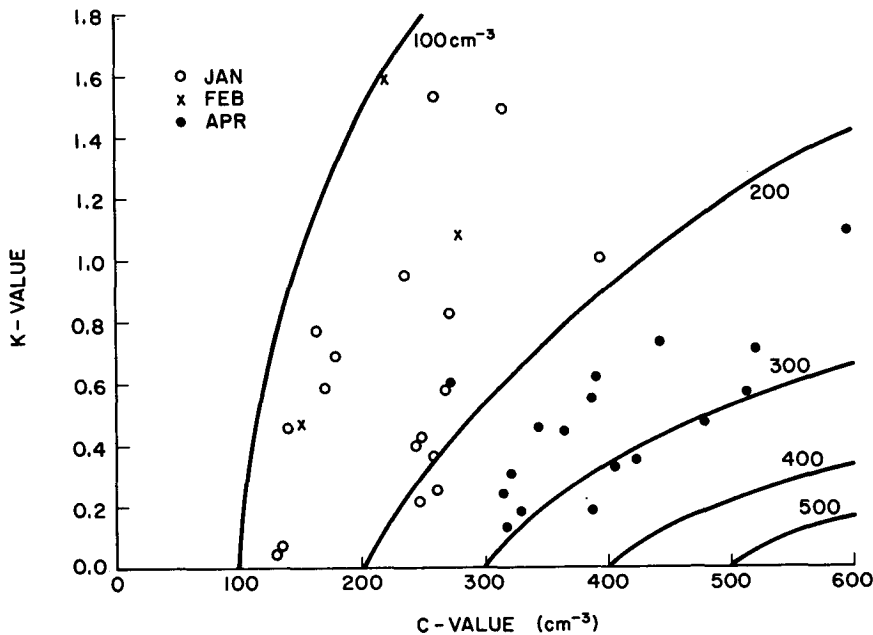


FIG. 14. C and k values for equations of the form $N = CS^k$ fitted to the CCN spectra measured during the winter of 1978-79. Lines represent droplet concentrations based on Twomey's (1959) equation for a 1 m s^{-1} updraft. Data are from ground-based samples in the Elk Mountain vicinity.

TABLE 4. Predictions of droplet concentrations from CCN measurements.

	Updraft speed (cm s^{-1})			
	50	100	150	200
Mean (cm^{-3})	177	207	243	266
Standard deviation	63	73	70	74

during the late morning and afternoon. The research aircraft N10UW sampled the cloud from 1415–1520 MST. During this time the cloud was rather shallow and contained some convective bubbles near the downwind edge. The cloud base was at 3.1 km and the top near 4.3 km. Horizontal extent of the cloud was $\sim 7 \times 10$ km with the longer axis perpendicular to the wind.

CCN measurements were taken at a rate of about one sample every hour from 1125 to 1718 MST. Predictions of droplet concentrations were calculated from these data, using a relation described by Twomey (1959) for updraft speeds of 25–100 cm s^{-1} , and are plotted on Fig. 15. A 20 min time lag was allowed to approximate air parcel transit time from the sampling site which was ~ 25 km upwind of the Observatory.

Droplet spectra were measured at the Observatory from 1011–2200 MST using the ASSP and CG. One minute averages of droplet concentrations from the ASSP varied from <100 to >200 cm^{-3} and are also plotted. The CG values were slightly higher than those measured by the ASSP but tracked those measurements well.

Data from the CG onboard N10UW are also plotted on Fig. 15. Droplet concentrations measured by

the ASSP along the flight path in the main portion of the cloud maintained fairly steady values. However, these were not plotted because of an instrument problem which causes us to suspect the actual values. The CG measurements are “spot” values, but are probably representative of the droplet concentrations well into the cloud.

The droplet concentrations measured from the Observatory followed variations in the CCN spectra predictions fairly well. However, the measurements obtained from N10UW were consistently higher than both. Aitken particle counts (for data source see Table 1) taken during the flight revealed considerable vertical structure of aerosol in the boundary layer. A turbid layer (based on these Aitken particle counts) was present at ~ 500 – 900 m AGL, near the top of the boundary layer. Within this turbid layer, Aitken particle counts were >1000 cm^{-3} , while above and below they were <100 cm^{-3} . Winds in the boundary layer were up to 10 m s^{-1} from 270° . They veered as height increased and within the mixed layer they were from 300° at 10 – 15 m s^{-1} . Above this, they turned more westerly and speed decreased. This suggests a different source for air within the turbid layer. A gradient in CCN concentration similar to that observed in Aitken particle counts could explain higher droplet concentrations aloft.

In this case CCN spectra obtained at the surface were not characteristic of those throughout the vertical extent of the cloud. The droplet concentrations measured at the Observatory suggest that parcels sampled there had their origin near the surface upwind. Data taken at higher levels in the cloud suggest that the aerosol in those portions of the cloud had different characteristics and origin.

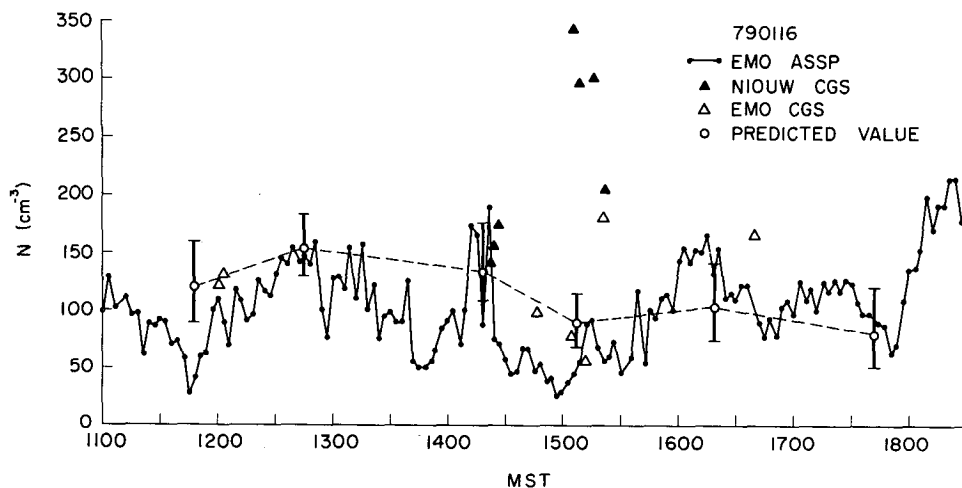


FIG. 15. Droplet concentrations plotted against time for 16 January 1979. Data sources are indicated. Circles represent an updraft of 50 cm s^{-1} , the vertical lines with bars represent the range of updrafts 25– 100 cm s^{-1} . A 20 min time lag was added to CCN data to account for transport time from sampling site to the Observatory.

8. Summary

Cap and orographic clouds at Elk Mountain form a fairly consistent data set useful for studies of nucleation, cloud structure, cloud seeding and for instrumentation analyses. Observed characteristics of water clouds agree well with predictions from CCN spectra and from a one-dimensional microphysical model. The structures of these clouds are similar to those described through measurements and predictions by Rauber and Grant (1981).

Average droplet concentrations measured from the mountaintop Observatory are $\sim 250\text{--}350\text{ cm}^{-3}$, in agreement with the wintertime continental CCN spectra measured in the area. Temporal variations in droplet numbers appear to follow variations in CCN. There does not appear to be any major variation in droplet concentrations through the (shallow) depths of the clouds.

Droplet spectra are typically narrow (dispersions ~ 0.2) and droplet sizes are small (mean diameters $7\text{--}10\ \mu\text{m}$). Liquid water contents measured from the Observatory are generally $< 0.3\text{ g m}^{-3}$, and are below adiabatic values. Reasons for this may be loss of water to riming upwind of the Observatory or the uncertainty of air parcel origins (which may enter through the upwind edge rather than through the cloud base).

Convective elements are sometimes evidenced by visual appearance noted from the research aircraft. These are shallow and short lived and have little effect on water droplet measurements at the Observatory. We have observed bimodal droplet spectra aloft, especially near the tops of these bubbles, which may be an effect of mixing of cloudy air parcels with different origins (such as described by Warner, 1973).

Acknowledgments. This work has been supported by the National Science Foundation under Grant ATM-7717540. The faculty, staff and students who contributed to the research effort at Elk Mountain are acknowledged, especially David Rogers, who collected much of the data and helped with the manuscript, and Robert Black, who collected the 1979 CCN measurements.

REFERENCES

- Auer, A. H., Jr., 1968: Determination of condensation nuclei spectra and supersaturation values in Yellowstone National Park. *J. Rech. Atmos.*, **6**, 289–295.
- Baumgardner, D., and G. Vali, 1981: Empirical evaluation of airborne liquid water measuring devices. *Proc. Third WMO Sci. Conf. Weather Modification*, Vol. 1, Clermont-Ferrand, 373–380.
- Black, R. A., 1979: Cloud droplet concentrations and cloud condensation nuclei in Elk Mountain cap clouds. M.S. thesis, University of Wyoming, 107 pp.
- Braham, R. R., 1974: Information content of CCN spectra versus measurements at a single supersaturation. *Preprints Conf. Cloud Physics*, Tucson, Amer. Meteor. Soc., 9–12.
- Cooper, W. A., and J. D. Marwitz, 1980: Winter storms over the San Juan Mountains. Part II: Microphysical processes. *J. Appl. Meteor.*, **14**, 927–941.
- , and G. Vali, 1981: The origin of ice in wintertime cap clouds. *J. Atmos. Sci.*, **38**, 1244–1259.
- Davis, C. I., and A. H. Auer, Jr., 1974: Use of isolated orographic clouds to establish the accuracy of diffusional ice crystal growth equations. *Proc. Conf. Cloud Physics*, Tucson, Amer. Meteor. Soc., 141–147.
- Hobbs, P. V., and D. G. Atkinson, 1976: The concentrations of ice particles in orographic clouds and cyclonic storms over the Cascade Mountains. *J. Atmos. Sci.*, **33**, 1362–1374.
- Kelly, R. D., 1978: Condensation-freezing ice nucleation in wintertime orographic clouds. M.S. thesis, University of Wyoming, 88 pp.
- Knollenberg, R. G., 1981: Techniques for probing cloud microstructure. *Clouds: Their Formation, Optical Properties and Effects*, P. V. Hobbs and A. Deepak, Eds., Academic Press, 15–92.
- Rauber, R., and L. O. Grant, 1981: Supercooled water zones in stably stratified flow over a mountain barrier. *Preprints Second Conf. Mountain Meteorology*, Steamboat Springs, Amer. Meteor. Soc., 395–400.
- Rogers, D. C., and G. Vali, 1978: Summer climatology of aerosols and nuclei in the central high plains of the U.S. *Preprints Conf. Cloud Physics and Atmospheric Electricity*, Issaquah, Amer. Meteor. Soc., 25–30.
- , and M. K. Politovich, 1982: Contribution to CCN workshop report from University of Wyoming Group. *J. Rech. Atmos.*, **15**, 203–207.
- , D. G. Baumgardner and G. Vali, 1983: Determination of supercooled liquid water content by measuring rime rate. *J. Climate Appl. Meteor.*, **22**, 153–162.
- Saunders, C. P. R., 1978: Electrification experiments on Elk Mountain. *J. Geophys. Res.*, **83**, 5050–5056.
- Squires, P., and C. A. Gillespie, 1952: A cloud droplet sampler for use on an aircraft. *Quart. J. Roy. Meteor. Soc.*, **78**, 387–393.
- Twomey, S., 1959: The nuclei of natural cloud formation. Part II: The supersaturation in natural clouds and the variation in cloud droplet concentration. *Geophys. Pure Appl.* **43**, 243–249.
- Warner, J., 1973: The microstructure of cumulus cloud. Part IV: The effect in the droplet spectrum of mixing between cloud and environment. *J. Atmos. Sci.*, **30**, 256–261.
- Young, K. C., 1974: A numerical simulation of wintertime, orographic precipitation. Part I: Description of model microphysics and numerical techniques. *J. Atmos. Sci.*, **31**, 1735–1748.